DOE/ET-53088-502 IFSR #502

Excitation of Nonlinear Wake Field in a Plasma for Particle Acceleration

B. BREIZMAN,[a] D.L. FISHER,
P.Z. CHEBOTAEV,[a] AND T. TAJIMA
Institute for Fusion Studies
The University of Texas at Austin
Austin, Texas 78712

June 1991

[a]Institute of Nuclear Physics, 630090 Novosibirsk, U.S.S.R.

EXCITATION OF NONLINEAR WAKE FIELD IN A PLASMA FOR PARTICLE ACCELERATION

B.N. Breizman, T. Tajima, D.L. Fisher, and P.Z. Chebotaev
Institute for Fusion Studies
The University of Texas at Austin
Austin, Texas 78712
and
Institute of Nuclear Physics, 630090 Novosibirsk, USSR

ABSTRACT

Excitation of large amplitude wake fields in a plasma for acceleration of particles is theoretically and computationally considered. The wake electric field can be generated either by short laser pulses or charged particle (electrons) beam pulses. We treat both cases from a unified point of view and compare them. In two (or three) dimensional investigations, the wake causing agencies are treated as rigid, while in the one dimensional cases the feedback of the wake field on the driving pulse is accounted for fully kinetically and relativistically. We elucidate transverse and longitudinal wavebreaking effects, nonlinear wake field effects, pulse shaping, multiple pulses, the coherency length of wake fields and comparison of laser and electron beam pulses.

INTRODUCTION

A promising way of achieving super high accelerating gradients for future linear colliders is the use of a plasma-based accelerator in which a plasma wave is driven either by a short laser pulse or a relativistic electron beam. These schemes are known now as the laser wake field accelerator (LWFA) and the plasma wake field accelerator (PWFA). Some of the early ideas on this have been introduced by Veksler in 1956 (see Ref. 1). In Ref. 2 a laser pulse was introduced to induce a wake, as the laser pulse is capable of creating a fast phase velocity. Some later papers went back to the original charged particle ideas. The electron beam version of PWFA was proposed in the theoretical paper,[3,4] and its basic principles have also been tested experimentally.[5] Recently, an enhanced accelerating gradient has been obtained in a new experiment,[6] and there are at least two more experiments[7,8] proposed with substantially increased parameters.

To address an experimental situation, theory of either the LWFA or the PWFA is desirable to be both three dimensional and nonlinear. Three dimensional effects are especially important when the wake field is excited by an electron beam, since the transverse dimensions of the driving beam are typically less than its length. In addition, the self fields of an ultrarelativistic electron beam have predominantly transverse components. The nonlinearity of a plasma is also an important issue in the whole problem, since there is a nonlinear limitation on the amplitude of the plasma wave excited by the beam. Though the above arguments had long been commonly accepted, the theory developed so far has

been often limited by using either a linear approximation or a one-dimensional model. The two objectives of this paper are to develope a simple fluid model for analytical and numerical study of the nonlinear dynamics of a three dimensional wake field and to present related fully self-consistent computer simulations for a one dimensional kinetic model.

When solving the general wake field problem, one has to take into account both the nonlinearity of the plasma and the deformation of the driver. However, in the ultrarelativistic limit the driver may be assumed to be "rigid", i.e. the back effect of the excited field on the driver can be neglected (at least as a first approximation).

The nonlinear limitation on the accelerating gradient stems from Langmuir wave breaking. As it was shown for the one-dimensional case in Ref. 9, the wave breaking is characterized by a finite threshold amplitude of the electric field. In contrast to this, the wave will always eventually break even for small amplitude waves in the three-dimensional case (see Ref. 9). With decreasing wave amplitude the wave breaking is delayed in time, but it does not disappear. In the context of the problem, it means that that the length of the "laminar wake", where the field structure is suitable for particle acceleration, depends on the accelerating gradient. As the gradient increases, the length become shorter, hence, the question arises as how large a gradient can be achieved with a acceptable length of the laminar wake.

This particular question may be addressed within the fluid description of plasma electrons on the background of immobile plasma ions. As the velocity of the driver is very close to the velocity of light, all the fields and currents in a plasma are assumed to depend on the longitudinal coordinate z and time t in a combination $z - ct$, like in a travelling wave. This assumption is consistent with the fact that the plasma is unperturbed far ahead the leading edge of the driver because the group velocities of both electromagnetic and Langmuir waves are less than the driver velocity. An additional assumption is an axial symmetry of the problem.

In the three dimensional model the fluid approximation is used and the driver acts on the plasma; however, there is no feedback on the driver. This "rigid" driver approximation which allows an important three dimensional analysis is valid over short distances. The one dimensional kinetic model gives the self-consistent interaction of the driver with the plasma at the cost of reduction in dimensions. This simulation can test the rigidity approximation

The fluid model that we use reduces a physically three dimensional problem to a mathematically one dimensional one for which a numerical solution can be obtained easily. A simple fluid code which solves this problem can be further combined with a much more sophisticated kinetic code to describe the dynamics of the driving beam on a time scale determined by the distortion of the driver. This second time scale is much longer than the period of plasma wave. The combined code will certainly be less time consuming than a fully kinetic code.

BASIC EQUATIONS
Electron Driver

Derivation for an electron beam driver will be initially investigated, with modifications then given for a laser driver. A set of equations to be solved includes a relativistic equation of motion for plasma electrons

$$\frac{\partial \mathbf{p}}{\partial t} + (\mathbf{v}\nabla)\mathbf{p} = -e\left(\mathbf{E} + \frac{1}{c}[\mathbf{v}\times\mathbf{H}]\right) , \tag{1}$$

wherein $\mathbf{v} = c\mathbf{p}/\sqrt{p^2 + m^2c^2}$, a continuity equation

$$\frac{\partial n}{\partial t} + \mathrm{div}\,(n\mathbf{v}) = 0 \tag{2}$$

and Maxwell equations:

$$\mathrm{rot}\,\mathbf{H} = \frac{4\pi}{c}\mathbf{j} + \frac{1}{c}\frac{\partial \mathbf{E}}{\partial t} , \tag{3}$$

$$\mathrm{rot}\,\mathbf{E} = -\frac{1}{c}\frac{\partial \mathbf{H}}{\partial t} . \tag{4}$$

A total current $\mathbf{j}$ in Eq. (3) is the sum of a plasma electron current

$$\mathbf{j}_p = -en\mathbf{v} \tag{5}$$

and a current of a driving beam $\mathbf{j}_b$. For a rigid axisymmeric beam, $\mathbf{j}_b$ is directed along the z-axis of a cylindrical coordinate system (r, φ, z) and is a given function of r and $t - z/c$. For the particular computational runs we take a gaussian radial profile of the beam. It is convenient to rewrite Eqs. (1)-(4) in a dimensionless form by introducing new (dimensionless) variables that are marked by primes and defined by the following transformations:

$$t \Rightarrow \sqrt{\frac{m}{(4\pi n_0\theta^2)}}\,t' \ ; \ \mathbf{r} \Rightarrow \sqrt{\frac{mc^2}{(4\pi n_0 e^2)}}\,\mathbf{r}' \ ; \ \mathbf{p} \Rightarrow mc\mathbf{p}' \ ; \ \mathbf{v} \Rightarrow c\mathbf{v}' \ ;$$

$$n \Rightarrow n_0 n' \ ; \ \mathbf{j} \Rightarrow -en_0 c\mathbf{j}; \ ; \ \mathbf{E} \Rightarrow -\sqrt{4\pi n_0 mc^2}\,\mathbf{E} \ ; \ \mathbf{H} \Rightarrow -\sqrt{4\pi n_0 mc^2}\,\mathbf{H}' \ . \tag{6}$$

Here, n_0 is the unperturbed plasma density and the fields are normalized to the wavebreaking value $E_0 \equiv m\omega_p c/e$. In what follows we omit the prime at a dimensional variable. By assuming an axisymmetric travelling wave dependence $(r;\ t - z/c)$ for all the functions we eliminate z-derivatives from Eqs. (1)–(4). We also introduce new unknown functions V_z, V_r and N that are related to v_z, v_r and n by equations

$$V_z \equiv \frac{v_z}{1 - v_z} , \quad V_r \equiv \frac{v_r}{1 - v_z} , \quad N \equiv n(1 - v_z) .$$

Finally, Eqs. (1)–(4) take the form

$$\frac{\partial}{\partial t} V_r + V_r \frac{\partial}{\partial r} V_r = \sqrt{1 + 2V_z - V_r^2} \left[(1 + V_z - V_r^2)(E_r - H) + H + V_r E_z \right] , \quad (7)$$

$$\frac{\partial}{\partial t} V_z + V_r \frac{\partial}{\partial r} V_z = \sqrt{1 + 2V_z - V_r^2} \left[(1 + 2V_z) E_z + V_r H - V_r V_z (E_r - H) \right] , \quad (8)$$

$$\frac{\partial}{\partial t} N + \frac{1}{r} \frac{\partial}{\partial r} (r N V_r) = 0 , \quad (9)$$

$$\frac{\partial}{\partial t} (E_r - H) = -N V_r , \quad (10)$$

$$\frac{\partial}{\partial r} E_z = N V_r , \quad (11)$$

$$\frac{\partial}{\partial r} \frac{1}{r} \frac{\partial}{\partial r} (rH) = \frac{\partial}{\partial t} (N V_r) + \frac{\partial}{\partial r} (N V_z) + \frac{\partial}{\partial r} j_b . \quad (12)$$

For the driving beam current, j_b, in Eq. (12) we choose

$$j_b = j_0 \begin{cases} \exp\left(-\dfrac{r^2}{2\sigma_r^2} - \dfrac{t^2}{2\sigma_-^2} \right) ; & t \le 0 \\ \exp\left(-\dfrac{r^2}{2\sigma_r^2} - \dfrac{t^2}{2\sigma_+^2} \right) ; & t \ge 0 \end{cases} \quad (13)$$

with the parameters j_0, σ_r, σ_-, and σ_+ that determine a beam-to-plasma density ratio (j_0), beam radius (σ_r) and the widths of the beam leading edge (σ_-) and trailing edge (σ_+) measured in units of the plasma collisionless skin depth.

By analyzing the solution of Eqs. (7)–(12) one can, in principle, find the optimum values for the parameters j_0, σ_r, σ_-, and σ_+ to maximize the plasma wake field. Since the complete analysis of the solution is rather difficult we will restrict ourselves with a more practical problem of outlining a relevant range of parameters for creating experimentally the wake field of the order of hundreds GeV/m.

Laser Driver

We will model the laser pulse in the plasma by the ponderomotive force it produces, otherwise the electromagnetic fields of the laser pulse are ignored. This gives the "rigid" laser pulse with all the fields in the basic equations due only to the plasma. Effects of the feedback of wakefields on the laser pulse have been treated by a fluid approach, including the pump depletion in Ref. 10. A laser pulse with a radial profile will produce a radial and axial ponderomotive force

$$\mathbf{F}_p = -\frac{m}{2} \nabla \left(v_{osc}^2 \right) , \quad (14)$$

where $v_{\rm osc} = eE_{\rm laser}/m\omega_{\rm laser}$ is an electron oscillatory velocity in the laser field. A relativistic generalization can be done.

This force is to be included in the equation of motion for plasma electrons

$$\frac{\partial \mathbf{p}}{\partial t} + (\mathbf{v}\nabla)\mathbf{p} = -e\left(\mathbf{E} + \frac{1}{c}[\mathbf{v}\times\mathbf{H}]\right) + \mathbf{F}_p \tag{15}$$

where the fields are only those due to the plasma.

The normalized force becomes

$$\mathbf{F} \Rightarrow \sqrt{4\pi n_0 m c^2 e^2 \mathbf{F}}\ , \tag{16}$$

Then the dimensionless equations (7) and (8) become

$$\frac{\partial}{\partial t}V_r + V_r\frac{\partial}{\partial r}V_r = \sqrt{1+2V_z-V_r^2}\ \left[(1+V_z-V_r^2)(E_r - H + F_r)\right.$$
$$\left. + H + V_r(E_z+F_z)\right]\ , \tag{17}$$

$$\frac{\partial}{\partial t}V_z + V_r\frac{\partial}{\partial r}V_z = \sqrt{1+2V_z-V_r^2}\ [(1+2V_z)(E_z+F_z) + V_r H$$
$$- V_r V_z(E_r + H + F_r)]\ . \tag{18}$$

The rest of the dimensionless equations (9)–(12) are as before, except that the beam current j_b is equal to zero.

LINEAR THEORY

Electron driver

A sufficient applicability condition for the linear theory is given by inequality $j_0 \ll 1$ for the electron beam or $F \ll 1$ for the laser pulse. With this condition being satisfied one can put $N = 1$ in Eqs. (10)–(12) to split off Eq. (9) and to rewrite the remaining equations in the form

$$\frac{\partial}{\partial t}V_r = E_r\ , \tag{19}$$

$$\frac{\partial}{\partial t}V_z = E_z\ , \tag{20}$$

$$\frac{\partial}{\partial r}E_z = V_r\ , \tag{21}$$

$$\frac{\partial}{\partial t}(E_r - H) = -V_r\ , \tag{22}$$

$$\frac{1}{r}\,\partial r\,(rH) = \frac{\partial}{\partial t}E_z + V_z + j_b\ . \tag{23}$$

We now substitute E_r, E_z and V_r in Eqs. (22) and (23) from Eqs. (19)–(21) to obtain

$$H = \frac{\partial}{\partial r}\left(\frac{\partial^2}{\partial t^2} V_z + V_z\right) \tag{24}$$

$$\frac{1}{r}\frac{\partial}{\partial r}(rH) = \frac{\partial^2}{\partial t^2} V_z + V_z + j_b \ . \tag{25}$$

It follows from Eqs. (24) and (25) that a vector potential A given by

$$\frac{\partial^2}{\partial t^2} V_z + V_z = A \tag{26}$$

satisfies the equation

$$\frac{1}{r}\frac{\partial}{\partial r} r \frac{\partial}{\partial r} A - A = j_b \ , \tag{27}$$

After solving this equation the longitudinal electric field E_z can be found from Eqs. (20) and (26):

$$E_z(r;t) = \int_{-\infty}^{t} A(r;t')\cos(t-t')dt' \ . \tag{28}$$

Equation (28) gives a sinusoidal wake field behind a driving beam

$$E_z(r;t)]E\cos(t+\psi) \tag{29}$$

with an amplitude E that depends on radius as

$$E = \sqrt{\left(\int_{-\infty}^{+\infty} A(r;t')\cos(t')dt'\right)^2 + \left(\int_{-\infty}^{+\infty} A(r;t')\sin(t')dt'\right)^2} \ . \tag{30}$$

For the current given by Eq. (13) the amplitude takes the form

$$E = j_0 R(r;\sigma_r)\sqrt{(Z_1(\sigma_-;\sigma_+))^2 + (Z_2(\sigma_-;\sigma_+))^2} \ , \tag{31}$$

wherein the following notations are introduced

$$R(r;\sigma_r) \equiv \left|\sigma_r^2 \int_0^\infty \frac{1}{k^2+1} \exp\left(\frac{k^2\sigma_r^2}{2}\right) J_0(kr)k\,kdk\right| \ . \tag{32}$$

$$Z_1(\sigma_-;\sigma_+) \equiv \sqrt{\frac{\pi}{2}}\left(\sigma_- \exp\left(-\frac{\sigma_-^2}{2}\right) + \sigma_+ \exp\left(-\frac{\sigma_+^2}{2}\right)\right) \ , \tag{33}$$

$$Z_2(\sigma_-;\sigma_+) \equiv \sigma_{-1}^2 F_1\left(1;\frac{3}{2};-\frac{\sigma^2}{2}\right) - \sigma_{+1}^2 F_1\left(1;\frac{3}{2};-\frac{\sigma_+^2}{2}\right) \ . \tag{34}$$

Here J_0 is a Bessel function and ${}_1F_1$ is a confluent hypergeometric function.

It follows from Eqs. (31) and (32) that the electric field E as a function of r reaches a maximum value on the beam axis. The dependence of $E(0)$ on σ_r is characterized by a monotonic function $R(0;\sigma_r)$ that is shown in Fig. 1. Since it is typical for an electron beam that both σ_- and σ_+ are larger than σ_r, we restrict σ_r by a condition

$$\sigma_r \leq \min(\sigma_-;\sigma_+) \ . \tag{35}$$

To maximize the wake field under this condition we will assume in what follows that

$$\sigma_r = \min(\sigma_-;\sigma_+) \ . \tag{36}$$

As Eq. (31) is symmetric with respect to σ_- and σ_+, it is sufficient for our purpose to consider the case $\sigma_+ \leq \sigma_-$. Shown in Fig. 2 is the dependence of the wake field on σ_+ with σ_+ given by Eq. (36) for the symmetric beam ($\sigma_- = \sigma_+$) and for the beam with a very long leading edge ($\sigma_- \Rightarrow \infty$). The positions of the maxima are almost the same in both cases ($\sigma_+ = \sigma_r \approx 1.3$), while the maximum values of E differ by a factor of 2. Namely, $E_{\max} \approx 0.8 j_0$ for the symmetric beam and $E_{\max} \approx 0.4 j_0$ for the asymmetric one. There is a simple qualitative argument for the existence of the maxima in Fig. 2. At small values of σ_+ the wake field is less than the maximum value because of a smaller number of particles in a driving beam. At a large values of σ_+ the field decreases because the beam switches on adiabatically so that the beam space charge can be neutralized by the plasma. By extrapolating the results of linear theory up to $j_0 = 0.5$ we would obtain a dimensionless wakefield to be 0.4 for the symmetric beam and 0.2 for the asymmetric beam.

With the normalization (6) we have for the above quantities in their dimensional form $j_0 = 0.5\, enc$, $E_{\max} = 0.4\, m\omega_p c/e$, and $E_{\max} = 0.2 m\omega_p c/e$. At a plasma density $10^{15}\,\mathrm{cm}^{-3}$ these numbers correspond to 1200 MeV/m and 600 MeV/m respectively. An optimal beam radius is equal to 0.22 mm for this density. The above values determine the characteristic scales for the parameters in our nonlinear numerical simulations.

Laser driver

In the linear approximation for the laser pulse Eqs. (17) and (18) become

$$\frac{\partial}{\partial t} V_r = E_r + F_r \ , \tag{37}$$

$$\frac{\partial}{\partial t} V_z = E_z + F_z \ . \tag{38}$$

We now define the electric potential ψ and the ponderomotive potential ϕ such that

$$E_r = \frac{\partial \psi}{\partial r} \ , \qquad E_z = \frac{\partial \psi}{\partial t} \ , \tag{39}$$

$$F_r = \frac{\partial \phi}{\partial r} \ , \qquad F_z = -\frac{\partial \phi}{\partial t} \ . \tag{40}$$

Since the force is derivable from a potential, there is no magnetic field in the linear approximation. From these and the original equations we get

$$\frac{\partial^2}{\partial t^2}\psi + \psi = \phi \ . \tag{41}$$

The solution for Eq. (41) is

$$\psi = \int_{-\infty}^{t} \phi(t';r)\sin(t-t')dt' \ . \tag{42}$$

The amplitude of the potential ψ depends on the ponderomotive potential. Assuming $f(t)$ to be an even function of t, we obtain

$$\text{ampl} = \max \int_{-\infty}^{\infty} \phi(t';r)\cos(t')dt' \ . \tag{43}$$

For a ponderomotive potential with a gaussian radial and longitudinal profiles

$$\phi = C\exp\left(\frac{-t^2}{2\sigma_z^2}\right)\exp\left(\frac{-r^2}{2\sigma_r^2}\right) \tag{44}$$

the amplitude becomes

$$\text{ampl} = \sqrt{2\pi}\,\sigma_z C\exp\left(-\frac{\sigma_z^2}{2}\right) \ . \tag{45}$$

The calculation of the force from this form of the laser pulse is valid only for nonrelativistic velocities of the plasma electrons. If the amplitude of the force is such that either the velocity of the electrons due to the electric field of the laser pulse or the velocity of the electrons in the plasma wave becomes comparable to the speed of light, then the force given above will not come from the gaussian form of the laser pulse. The corrections to the nonrelatistivic ponderomotive force have not been considered here.

COMPUTATIONAL RESULTS

Equations (7) to (12) from the 2-D problem with a rigid driver were solved numerically with a fluid code. We also used a fully relativistic 1-D kinetic code (see e.g. Ref. 11) to study the effects of particle velocity spread which is important for studying wave breaking. In this section we present the numerical results for both electron and laser drivers with various longitudinal profiles and intensities. The radial profile of the driver for all 2-D runs is chosen to be gaussian with $\sigma_r = \min(\sigma_-;\sigma_+)$ for the electron driver and $\sigma_r = \sigma_z$ for the laser driver. For the longitudinal gaussian half width σ we used the optimal value from linear theory of 1.3 c/ω_p for the electron pulse and 1 c/ω_p for the laser pulse. In the case of a rigid driver relativistic factorγ was not specified ($v = c$); for the one-dimensional kinetic case we put $\gamma = 20000$.

Initially we shall look at electron drivers starting with the single pulse driver. In Figs. 3-5 we present the results for various densities of the driving beam. In each of the figures the radial profiles of the wake field and focusing force correspond to the right end point of the longitudinal profiles. Fig. 3 corresponds to a beam peak density which is 20% of the plasma electron density. Although the plasma wave look linear (sinusoidal), it is actually in the weakly nonlinear regime as is evidenced by the form of the focusing force. Since we are dealing with accelerating relativistic particles, the focusing force is defined as the radial electric field minus the magnetic field. In the linear region, the focusing force's sign is always opposite the slope of the wakefield, however, in Fig. 3b we see that the focusing force becomes positive after about 2.4 radii. The radial profile of the longitudinal field in Fig. 3 has a gaussian-like form as expected in the linear regime.

Next we look at a beam density that is 40% that of the plasma density (Fig. 4). There are now indications of nonlinearity in both the longitudinal and radial structure. The longitudinal field now has a steepened trailing edge and doubling the current from 20% to 40% increased the maximum amplitude by more than a factor of two. The amplitude also drops off due to nonlinear phase mixing of the harmonics. The structure of the focusing force is definitely nonlinear showing regions of large focusing and defocusing. Also the radial profile of the longitudinal wakefield has a blunted top and steep dropoff after about one radius due to nonlinearity.

The last 2-D single gaussian bunch (Fig. 5) has a beam density that is 60% that of the plasma density. The longitudinal wakefield has a steep trailing edge with a decreasing amplitude due again to nonlinearity. Although the longitudinal field looks nonlinear it does not appear to be close to wave breaking. However, if we look at the radial profile there is a very sharp change in the focusing force and in the radial profile of the longitudinal field at about three-fourths of a radii. The wave is on the verge of wave breaking in the radial direction.

Now we look at the velocity distributions with the one dimensional kinetic code. Since the 1-D code has an infinite radius, we expect the maximum wakefield amplitude to be larger than that for a finite beam radius of the same beam to plasma density ratio. Fig. 6 shows the phase space and plasma wakefield for a beam density of 20%. The initial distortion in the first 10 c/ω_p is due to startup and is to be neglected since it is unphysical. We see that the density perturbation is slightly peaked showing a weak nonlinearity. However, there is no wavebreaking and heating of the plasma and the plasma wave has a sinusoidal structure with no decrease in amplitude. The peak amplitude of the longitudinal oscillation is as expected larger than that for the 2-D case with a finite radius.

Fig. 7 shows a very nonlinear plasma oscillation which almost immediately starts to break. The beam density is 60% that of the plasma. In the phase space plot we see a very pointed top and a heating of plasma electrons. The electrons with large momentum are trapped by the wake field and are accelerated by the longitudinal field. The initial amplitude of 1.4 mwpc/e is above the

nonrelativistic wave breaking limit of $1.0m\omega_p c/e$.

Figure 8 shows the 2-D results for a slowly ramped pulse composed of two half gaussian, one with a wide width and the other with a sharp drop. The maximum current is 60% with a half width of about 17 plasma wavelengths. This shape gives an enhancement by a factor of 2 over the linear theoretical prediction of $0.24m\omega_p c/e$ for the peak amplitude of the wake field. We see from Fig. 8c that inside the pulse the focusing force is always negative and the longitudinal field is very low. In the wake field there is the usual nonlinear flattening of the radial profile of the wakefield and the nonlinear distortion of the focusing force.

Figure 9 shows the 2-D results of 5 bunches all spaced one plasma wavelength apart. The beam density of each bunch is 10% that of the plasma. This shows that following bunch amplifies the pulse in a linear fashion, the peak amplitude growing linearly with the number of bunches which have amplified the wave. After the final bunch the amplitude reduces somewhat as the wave is now in the nonlinear regime. The radial profile also shows as before the nonlinear behavior of distorting the focusing force and radial profile of the longitudinal electric field. Careful inspection of the wakefield shows a progression from the linear regime of a sinusoidal wake field to that of the nonlinear wave with a steepened profile.

Now we look at the cases for the laser pulse. In Fig. 10 we have the ponderomotive potential of an amplitude $0.1mc^2$ with a half width σ of 1. This corresponds to the laser intensity I of $0.1I_0$, where $I_0 = (\frac{\omega}{\omega_p})^2 nmc^2$. This gives a wake field amplitude of $0.15m\omega_p c/e$ consistent with linear theory, however, from the radial profile of the focusing force we observe that we are entering the nonlinear regime.

Fig. 11 now shows definite nonlinearity in both the nonsinusoidal longitudinal wake field and in the radial profiles. The normalized amplitude of the ponderomotive potential of the laser force is now $0.3mc^2$ in this case. As discussed in the theory section, the assumption that this force models a gaussian pulse is in question since we are now in the relativistic region.

For the last 2-D case we have three laser pulses of normalized amplitude $0.1mc^2$ spaced one wavelength apart. As in the multiple electron bunch case we see an amplification of the wake field starting in the weakly nonlinear regime and ending in the strongly nonlinear regime. From the radial profiles we see that the wave is near wavebreaking.

For the 1-D cases we now look at a normalized ponderomotive potential of $0.1mc^2$ in Fig. 12. As expected the amplitude is larger than that of the finite radius case and is in the weak nonlinear region. We observe no wavebreaking or heating in this region.

Figure 13, with a normalized potential of $0.6mc^2$, shows definite nonlinearity in both the phase space and in the wakefield. The phase space diagram shows the wave starting to break after about 2 oscillations, with the harmonics starting to modulate the wave. After about 4 oscillations we see the transition to chaos and the heating of the plasma. Correspondingly we see the amplitude of the

wakefield decrease due to nonlinearity and noise introduced due to the heating. Also observed are electrons trapped by the wakefield and accelerated.

CONCLUSION

In this paper we considered the excitation of a nonlinear plasma wave for the wakefield acceleration of high energy particles. By using the two dimensional fluid model we calculate the maximum amplitude of a wake field driven by either "rigid" electron beams or a given laser pulse and study the dynamics of the wave steepening and approach to wavebreaking. We also studied a one dimensional kinetic model in which depletion of a driver is taken into account and which is capable of describing a plasma motion after wave breaking. We observed that in a two-dimensional problem the wave steepening and breaking can occur first in the radial profile and not in the longitudinal profile. The length of the "laminar" wave after the driver decreases with increasing amplitude of the wake field. However, one can produce the wake field close to the wave breaking limit and have it suitable for particle acceleration and focusing on a distance of a few wavelengths behind the driver. In particular the accelerating field of $0.6m\omega_p c/e$ is feasible. The amplitude and the structure of the excited field depends substantially on the shape of the driver. We observed a nonlinear amplification of the wake field by a factor of 2 for a driving electron beam with a gentle slope leading edge and a sharply cut trailing edge. It is shown that the field can be strongly enhanced by employing multiple drivers with a spacing equal to one wavelength. The electron beam driver and a laser driver of a similar shape produce comparable wake fields when

$$\frac{\langle v_{osc}^2 \rangle}{2c^2} \approx \frac{j_b}{enc} . \tag{46}$$

A simple fluid code presented in this paper can be further incorporated into a more sophisticated three dimensional kinetic code to describe the dynamics of the driver and accelerated particles over the distance comparable to the length of acceleration. This longer distance typically exceeds the plasma wavelength by several orders of magnitude and the driver does not remain rigid over such a length, though it can be assumed rigid over a few wavelengths. The combined code would be much faster than a fully kinetic code alone since a lot of time can be saved by calculating the fields on the intermediate steps from the fluid code with a locally rigid driver.

ACKNOWLEDGMENTS

The work was supported in part by the U.S. Department of Energy grant DE-FG05-80ET-53088, and in part by the University Research Association subcontract to UTA.

REFERENCES

1. V.I. Veksler, Proceedings of CERN Symposium of High Energy Accelerators and Pion Physics, Vol.1, CERN, Geneva (1956)

2. T. Tajima and J. M. Dawson, Phys. Rev. Lett. **43**, 267 (1979)

3. P. Chen, J.M. Dawson, R.W. Huff, and T. Katsouleas, Phys. Rev. Lett. **54**, 693 (1985).

4. R.D. Ruth, A. Chao, P.L. Morton, and P.B. Wilson, Particle Accelerators **20**, 171 (1985).

5. J.B. Rosenzweig, D.B. Cline, B. Cole, H. Figueroa, W. Gai, R. Wonecny, J. Norem, P. Schoessow, and G. Simpson, Phys. Rev. Lett. **61**, 98 (1988).

6. A. Ogata, in *Proceedings of International Topical Conference on Research Trends in Coherent Radiation Generation and Particle Accelerators*, February 11-13,1991, La Jolla, California.

7. B.N. Breizman, P.Z. Chebotaev, I.A. Koop, A.M. Kudryavtsev, V.M. Panasyuk, Yu.M. Shatunov, A.N. Skrinsky, and F.A. Tsel'nik, in *Proceedings of the 8th International Conference on High-Power Particle Beams* (BEAMS–90), July 2–5, 1990, Novosibirsk.

8. C. Joshi, private communication (1991).

9. J.M. Dawson, Phys. Rev. **113**, 383 (1959).

10. W. Horton and T. Tajima, Phys. Rev. A **34**, 4110 (1986).

11. T. Tajima, "Computational Plasma Physics" (Addison-Wesley, Redwood City, 1989).

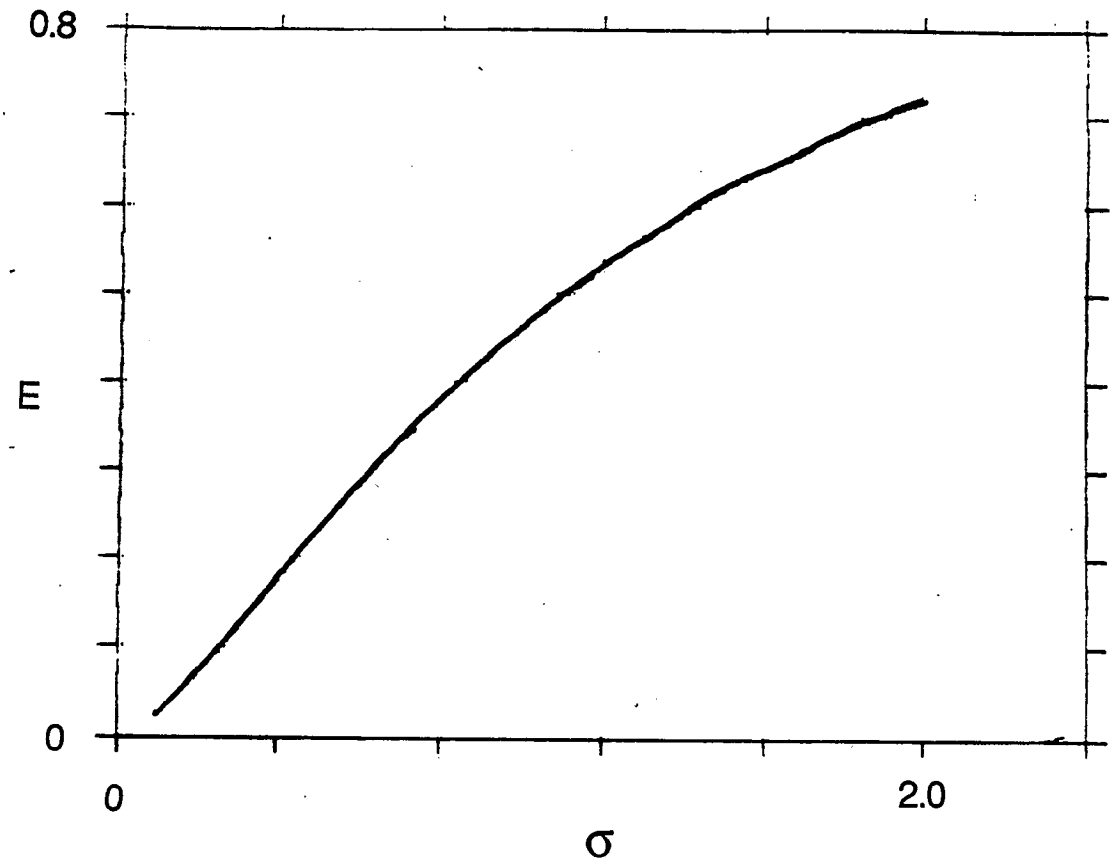

1. From equations (26) and (27) the dependence of the normalized wake field E at $r = 0$ as a function of given by $R(0, \sigma_r)$. E is normalized to $m\omega_p c/e$ and σ to c/ω_p.

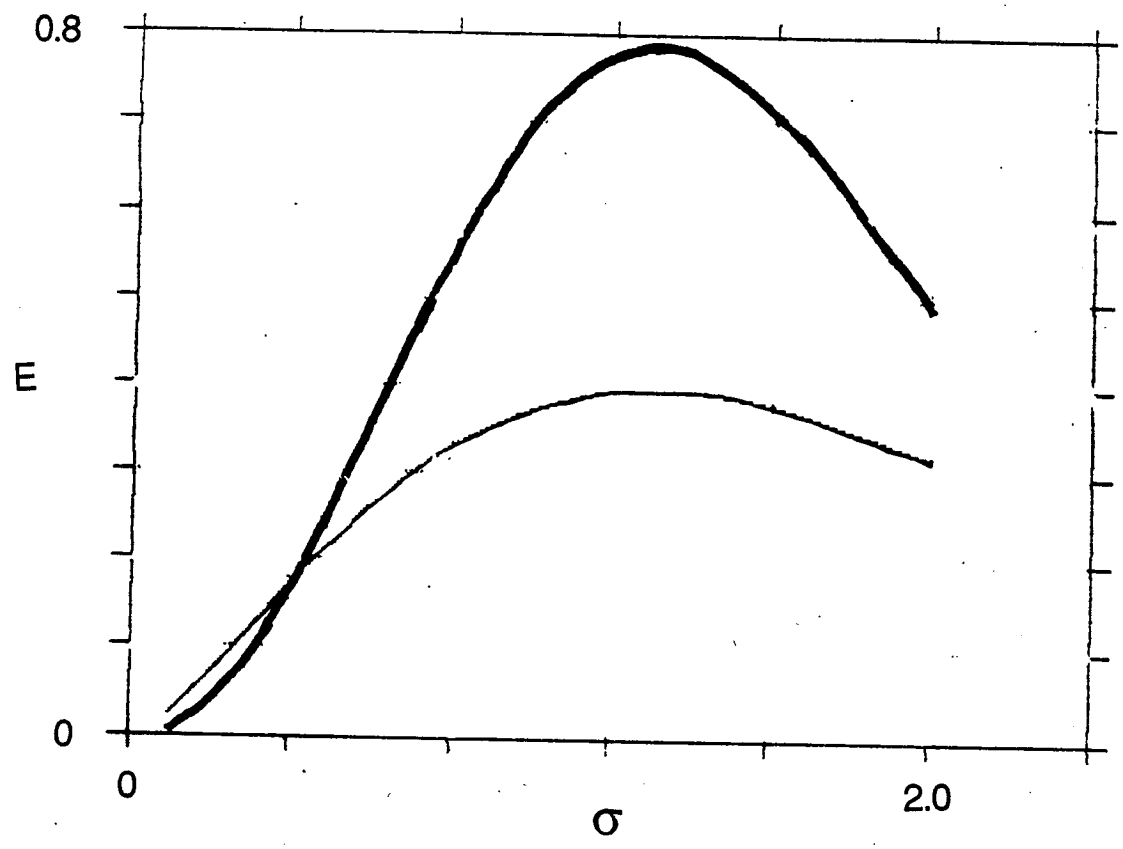

2. From equation (31) the dependence of the normalized wake field on normalized σ_r for a symmetric beam with $\sigma_- = \sigma_+$ (thick line) and for a beam with $\sigma_- \to \infty$ (thin line).

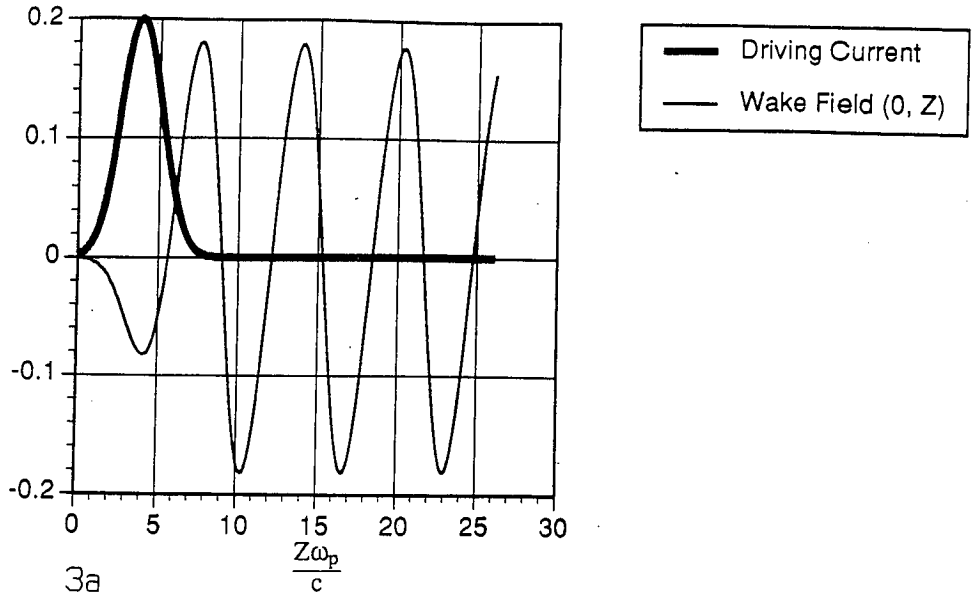

3a

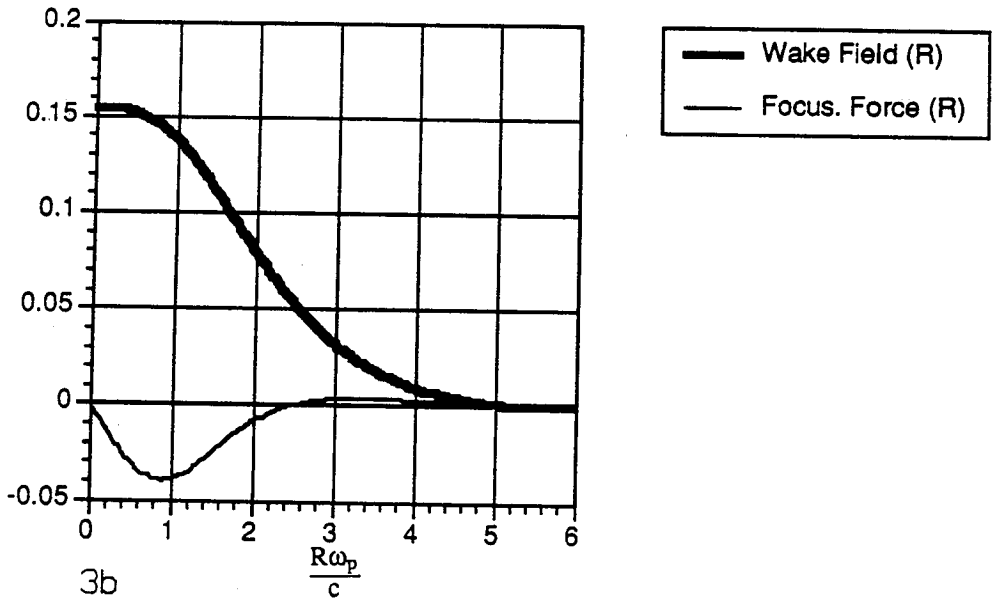

3b

3. Single gaussian electron beam, 2D fluid code. 3a — normalized beam current and normalized wake field for a beam peak current of $0.2nec$. 3b — normalized radial profiles of the wake field and the focusing force (radial electric field minus magnetic field) at the right end point of the wake field longitudinal profile. The wake field and the focusing force are normalized to $m\omega_p c/e$.

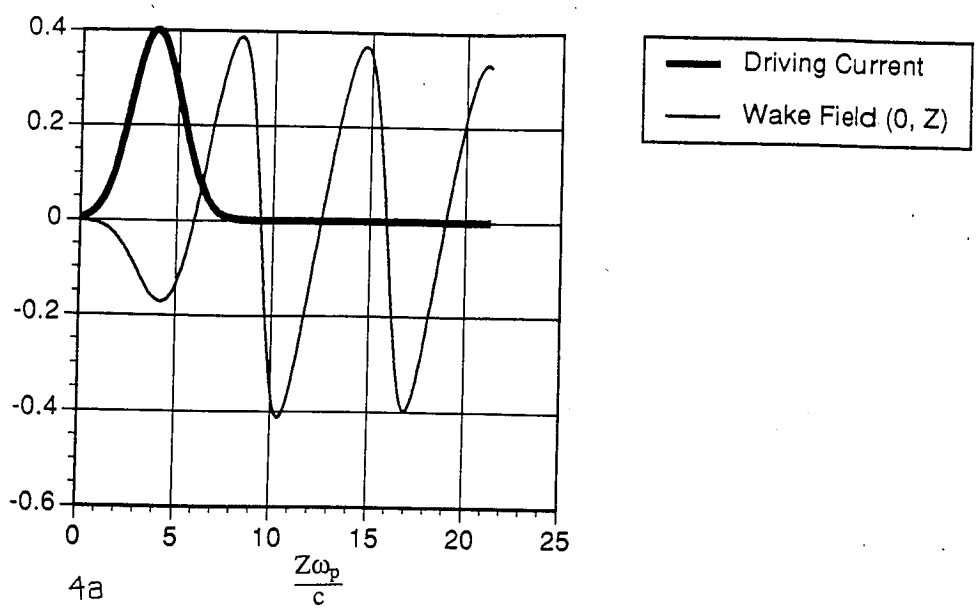

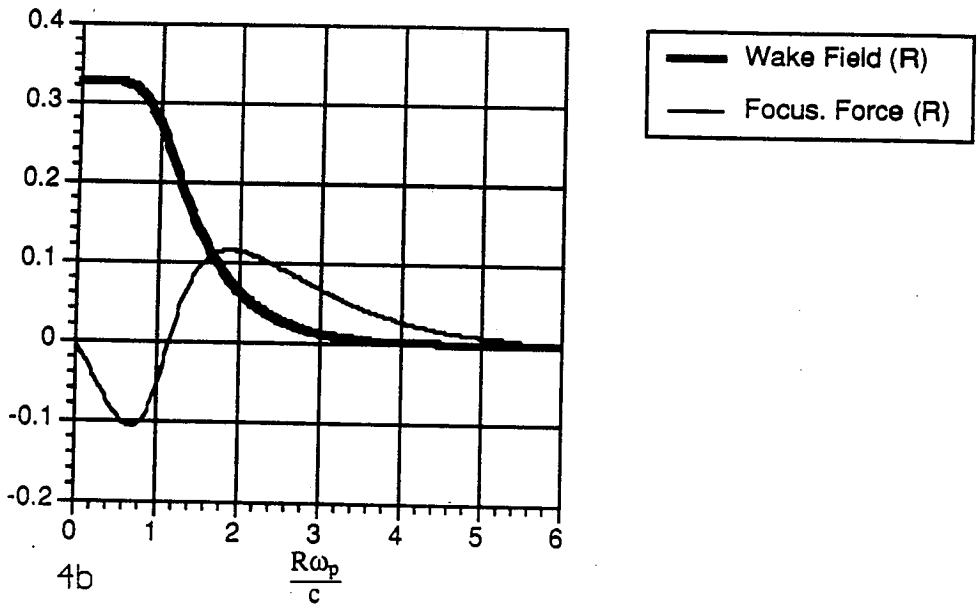

4. Same as Fig. 3 for beam current of 0.4.

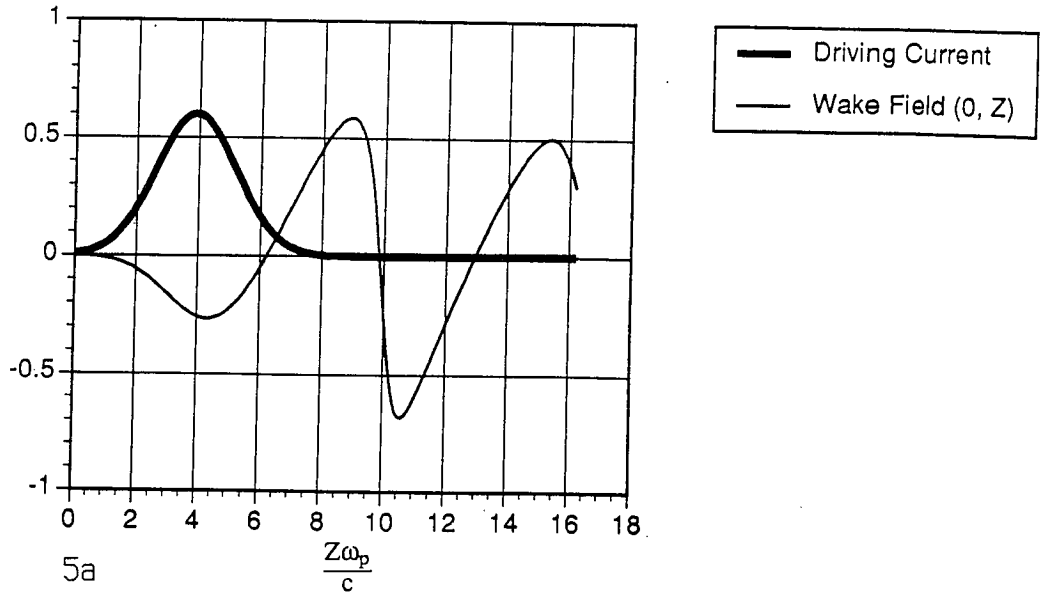

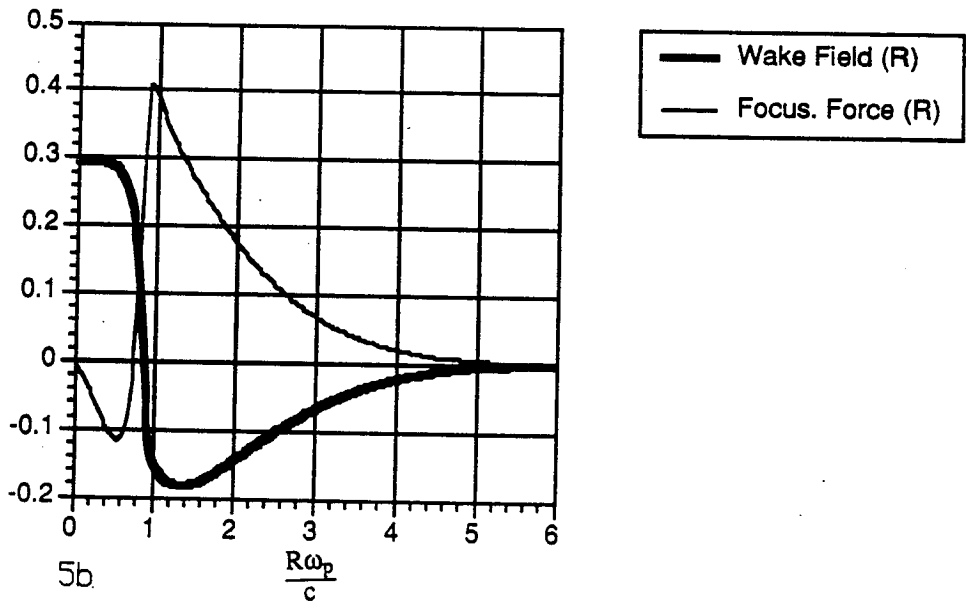

5. Same as Fig. 3 for beam current of 0.6.

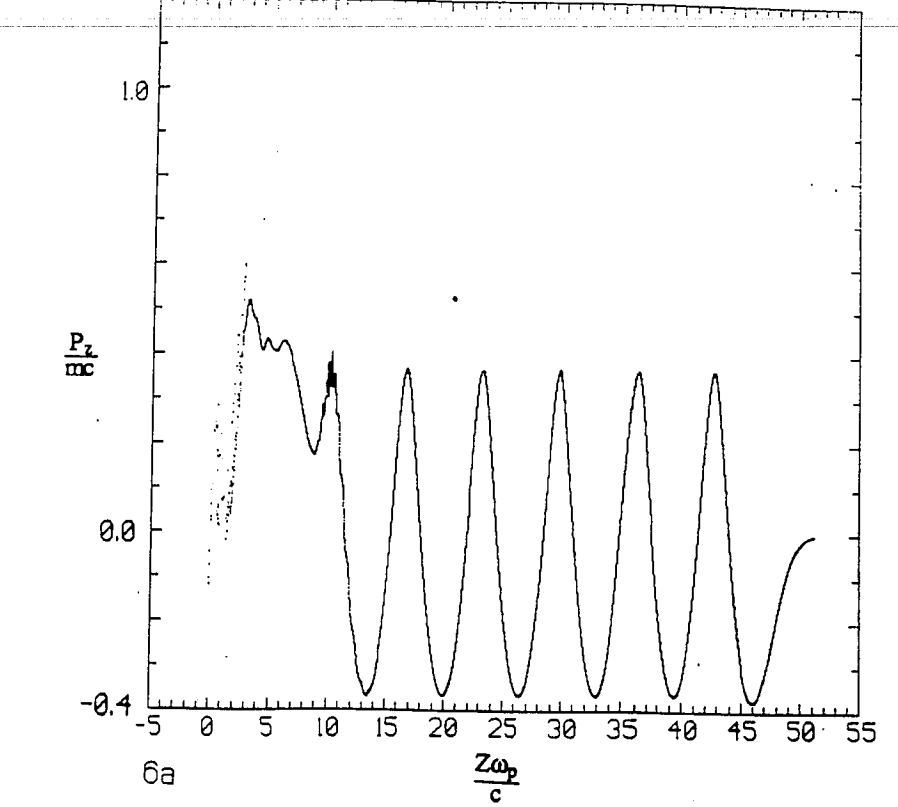

6a

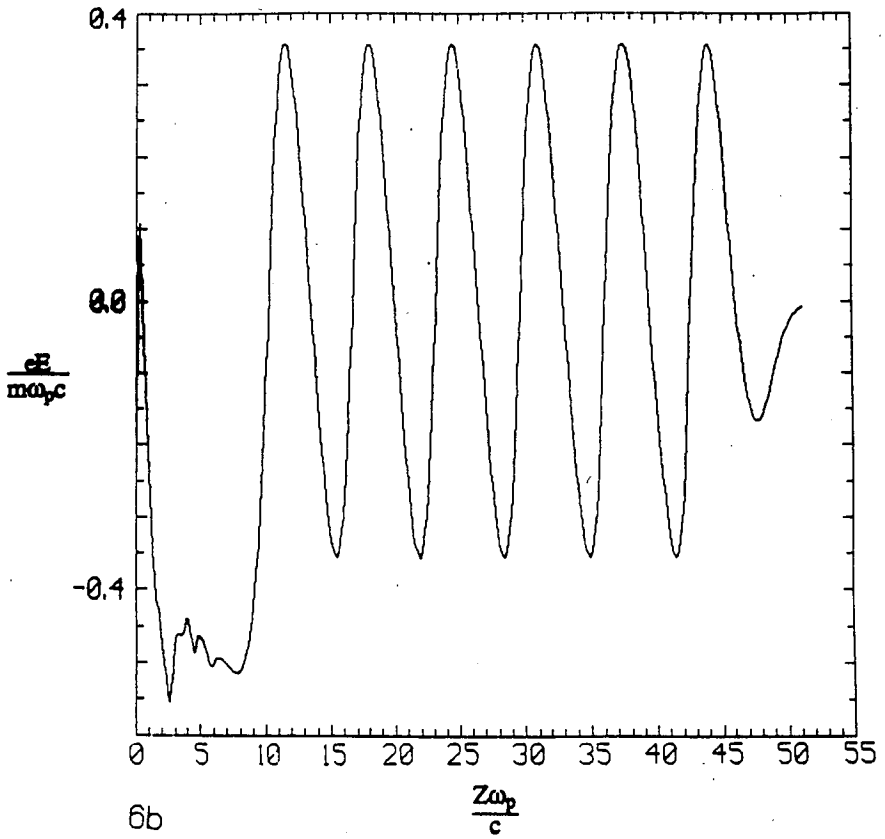

6b

6. Single gaussian electron beam, 1D kinetic code with normalized beam current of 0.2. 6a — phase space diagram and 6b — normalized wake field.

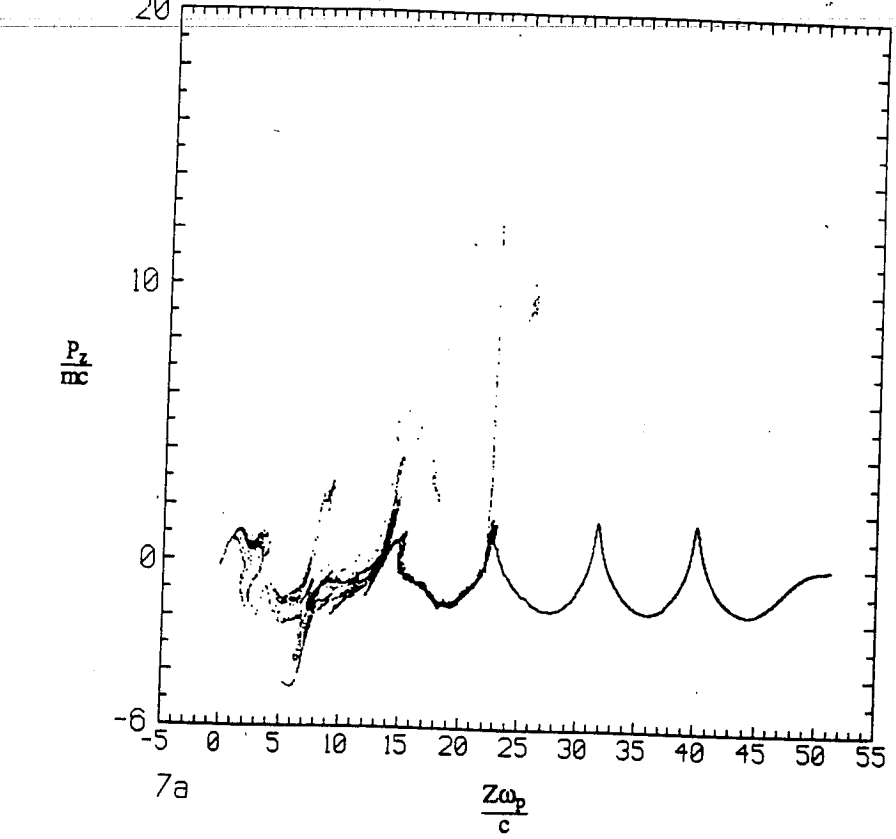

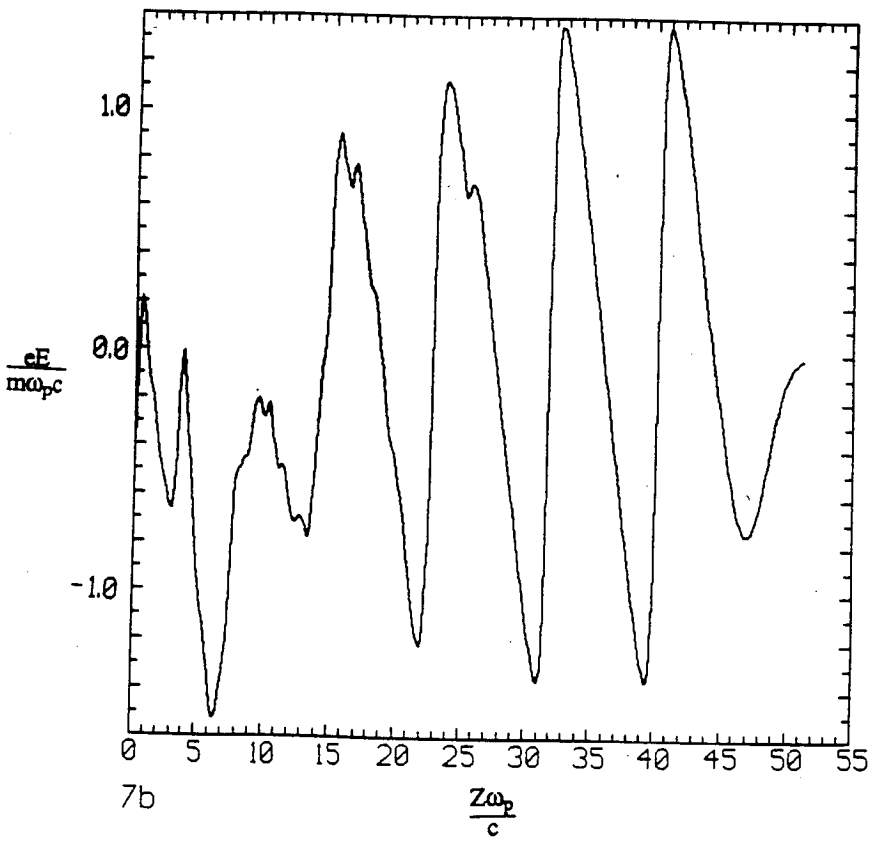

7. Same as Fig. 6 for beam current of 0.6.

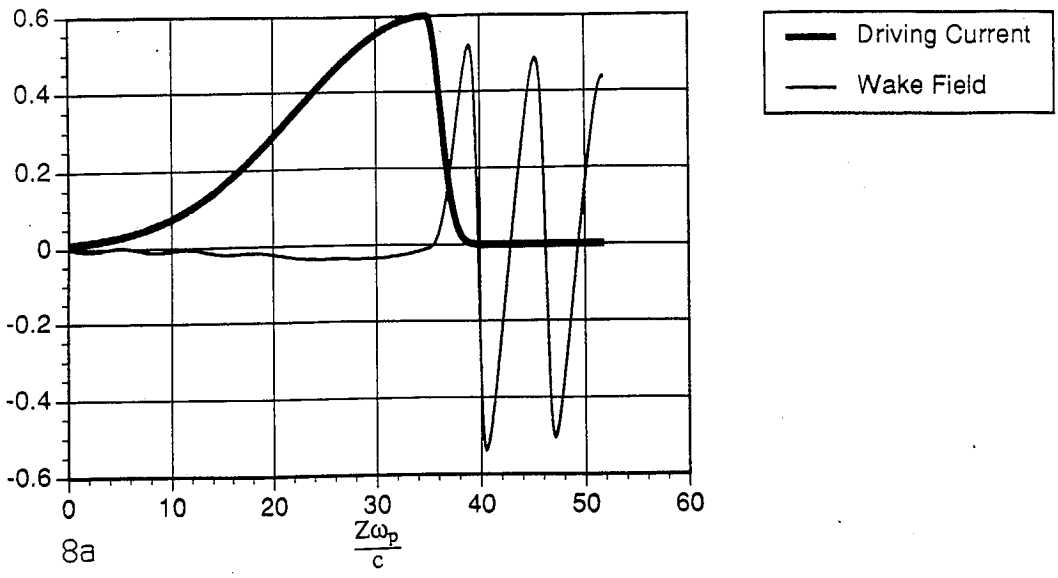

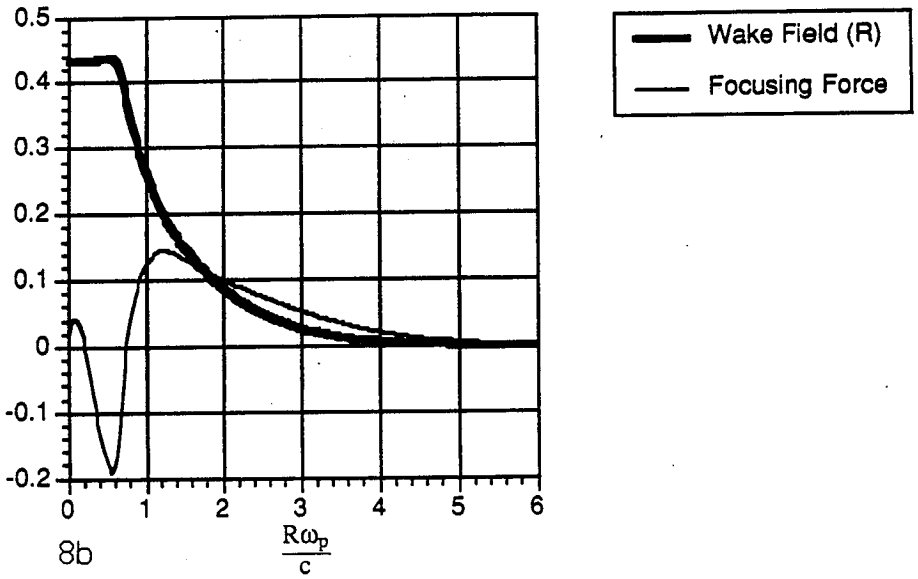

8. Slowly sloped electron beam with normalized peak current of 0.6, 2D fluid code. 8a — normalized driving beam and wake field. 8b — normalized radial profile of the wake field and focusing force at the right end point of the wake field longitudinal profile. 8c — normalized radial profile of the wake field and focusing force at the peak of the driving beam.

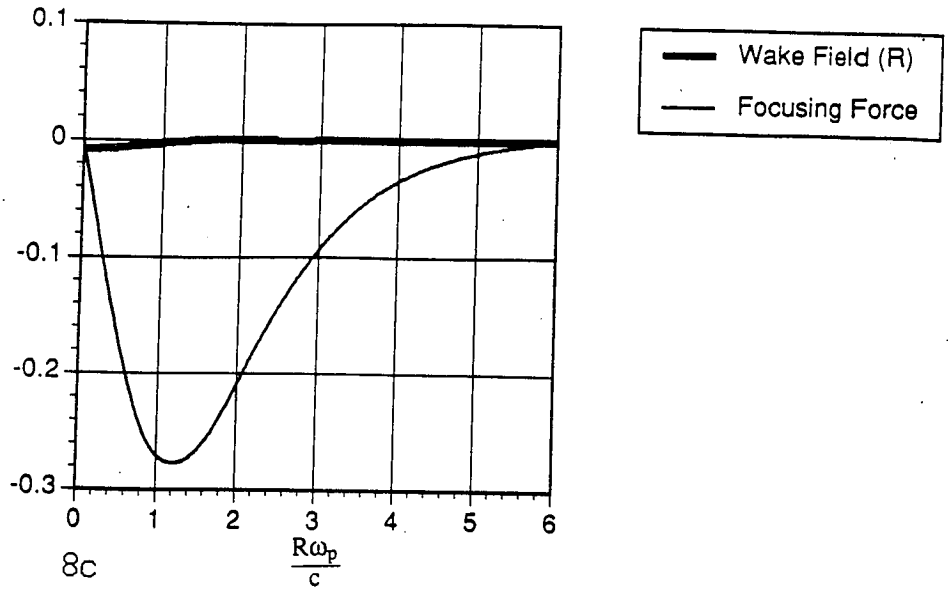
0.1
0
-0.1
-0.2
-0.3
0
1
2
3
4
5
6
$\frac{R\omega_p}{c}$
Wake Field (R)
Focusing Force

8c

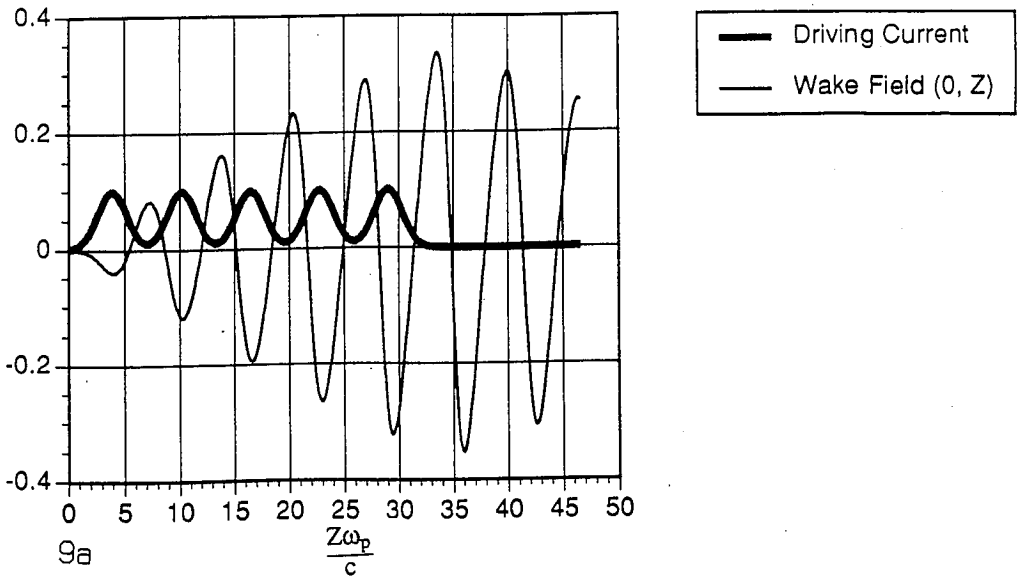

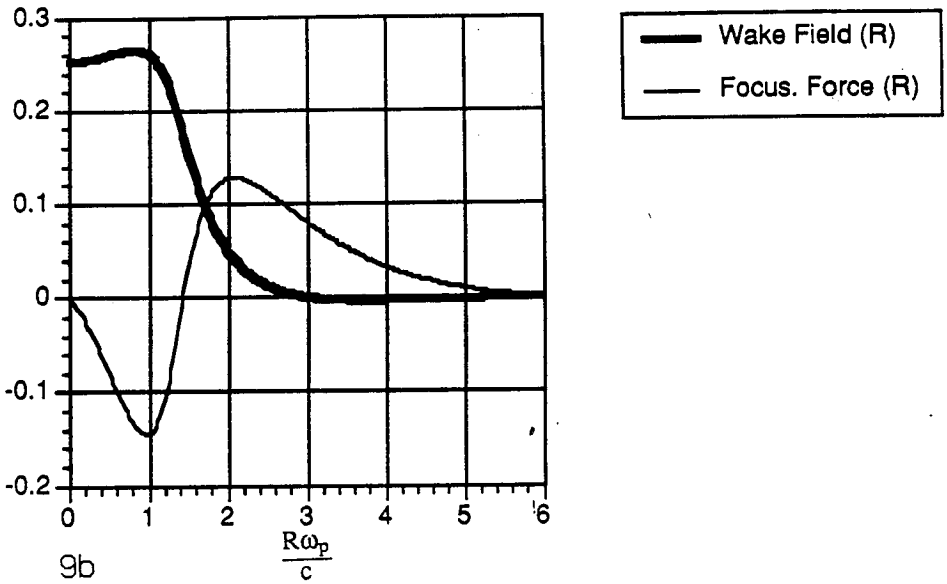

9. Five electron beams spaced one plasma wavelength apart each with current of 0.1. 9a — normalized driving beam current and wake field. 9b — normalized radial profiles of the wake field and focusing force at the right end point on wake field longitudinal profile.

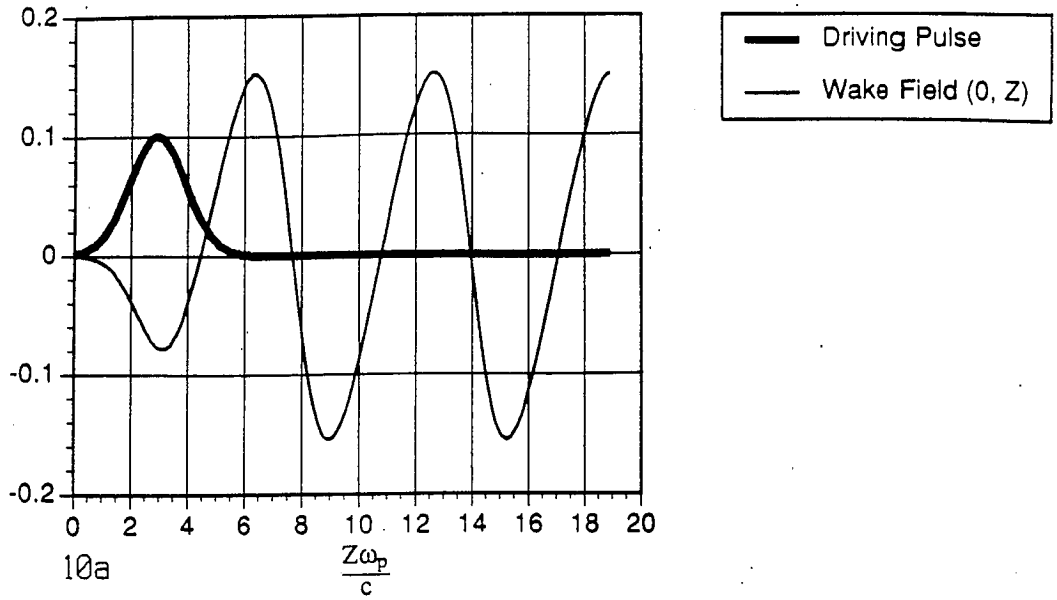

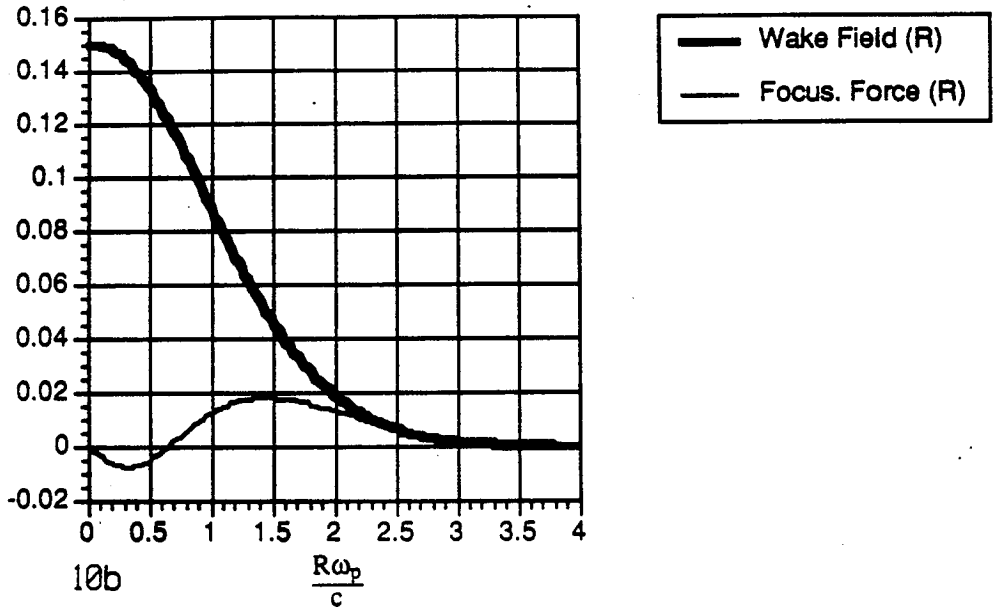

10. Gaussian laser pulse with normalized ponderomotive potential amplitude of $0.1mc^2$. 2D fluid code. 10a — normalized driving pulse and wake field. 10b — normalized radial profile of wake field and focusing force at the right end point on the wake field.

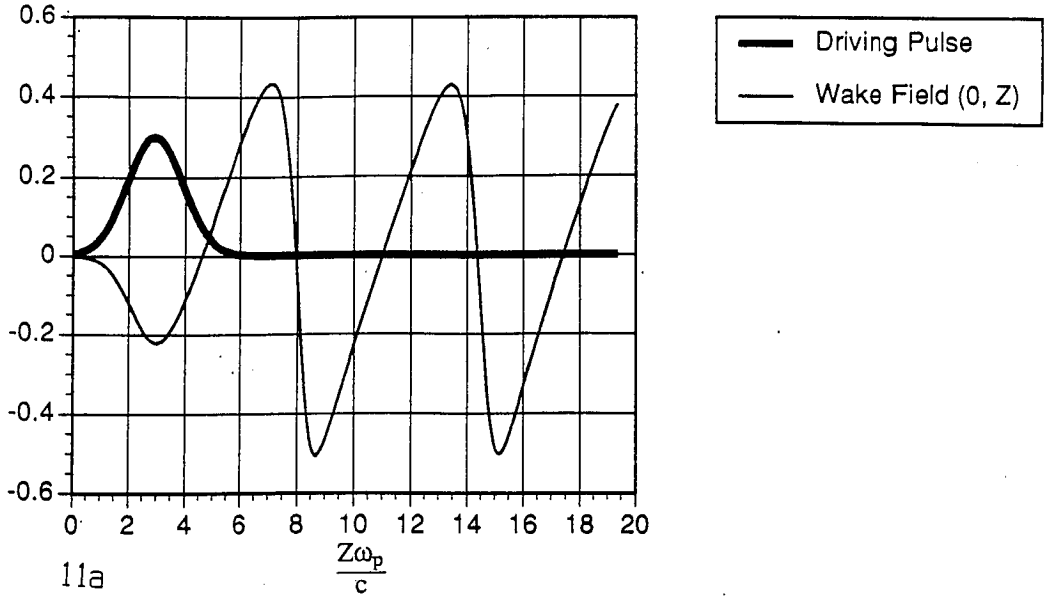

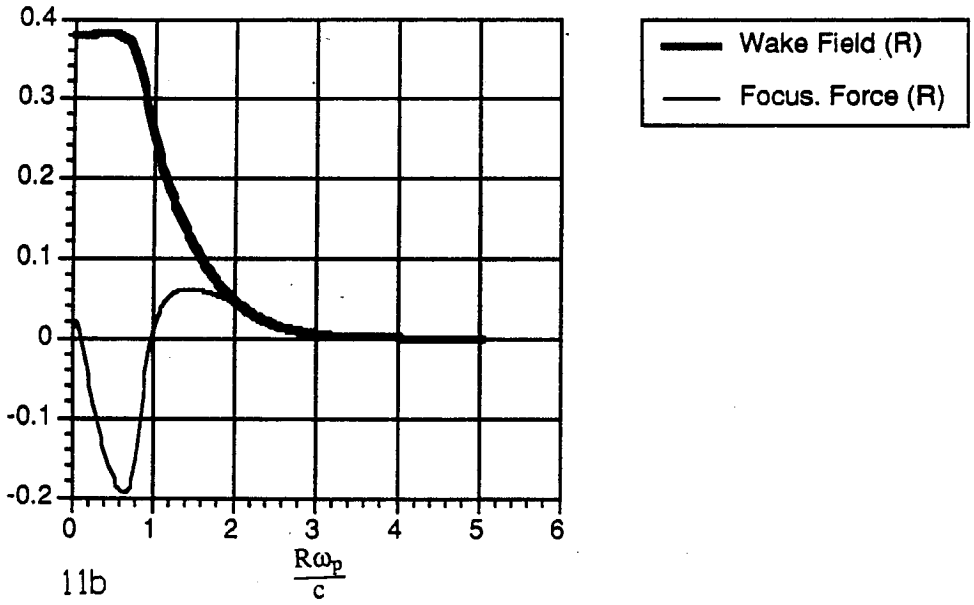

11. Same as Fig. 10 for a normalized pulse amplitude of $0.3mc^2$.

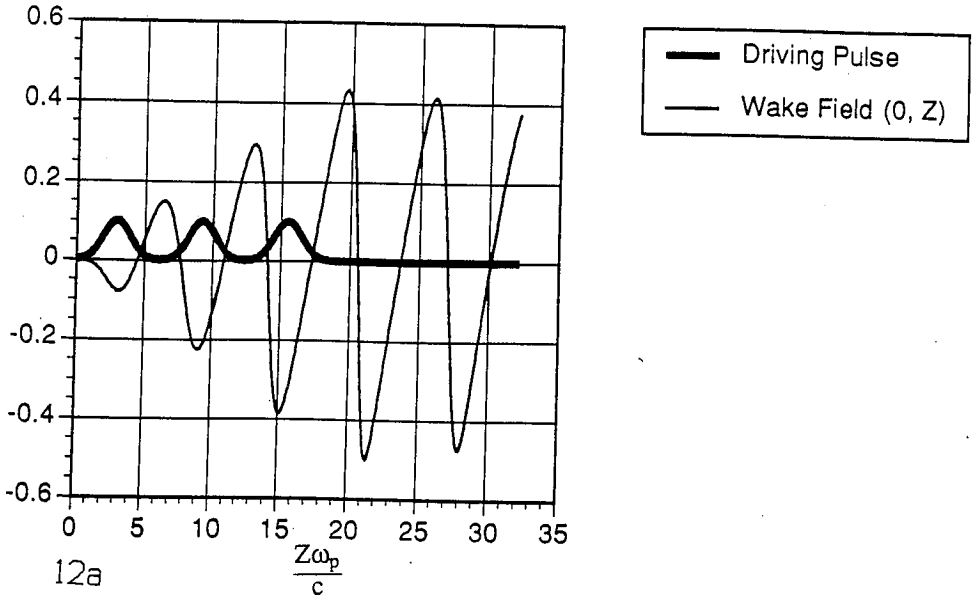

12a

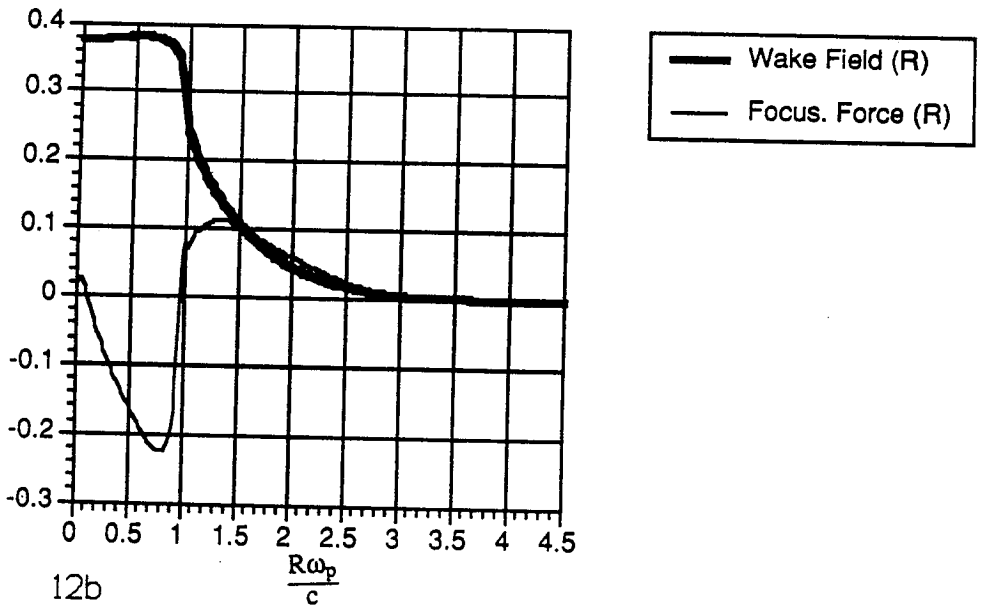

12b

12. Same as Fig. 10 for three laser pulses spaced one plasma wave length apart, each with normalized amplitude $0.1mc^2$.

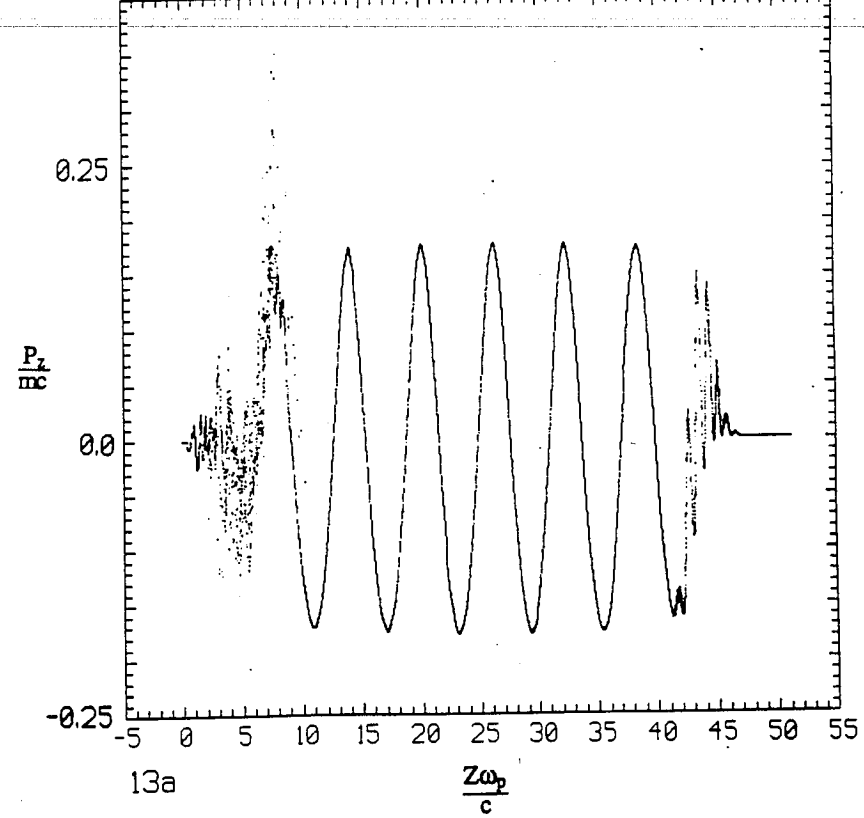

13a

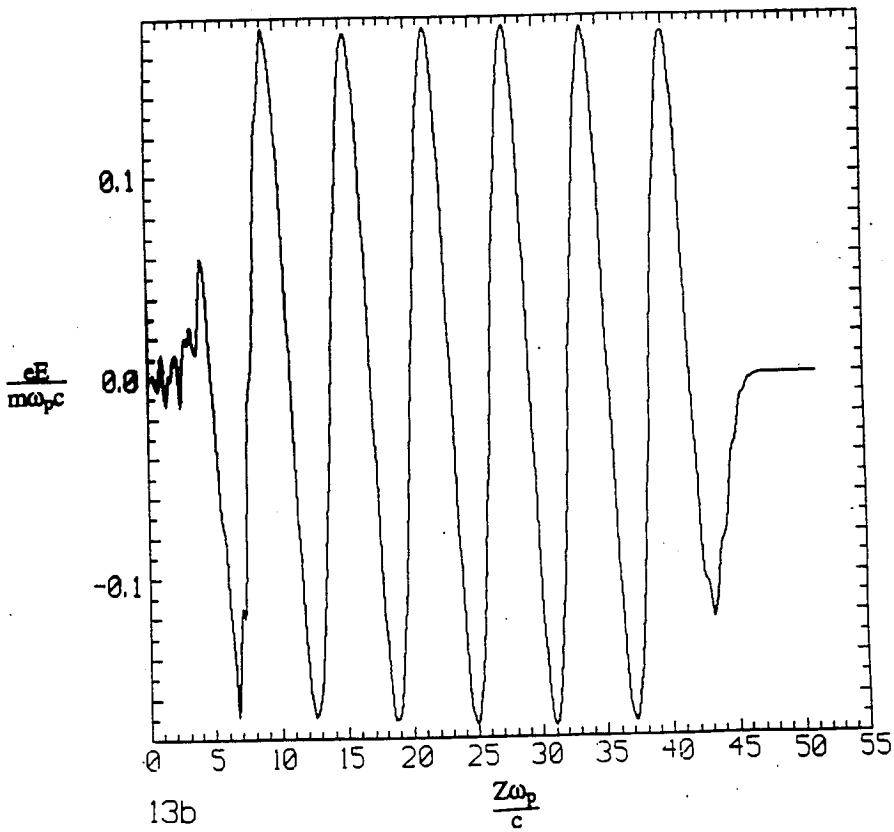

13b

13. Single gaussian laser pulse with normalized amplitude of $0.1mc^2$, 1-D kinetic code.13a — phase space plot. 13b — normalized wake field.

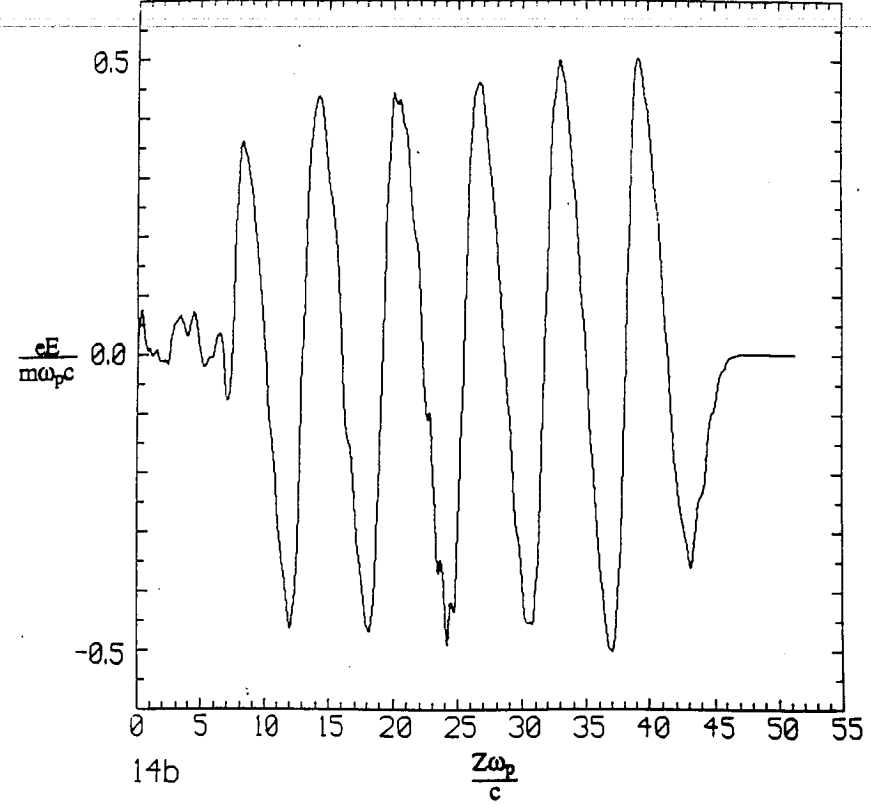

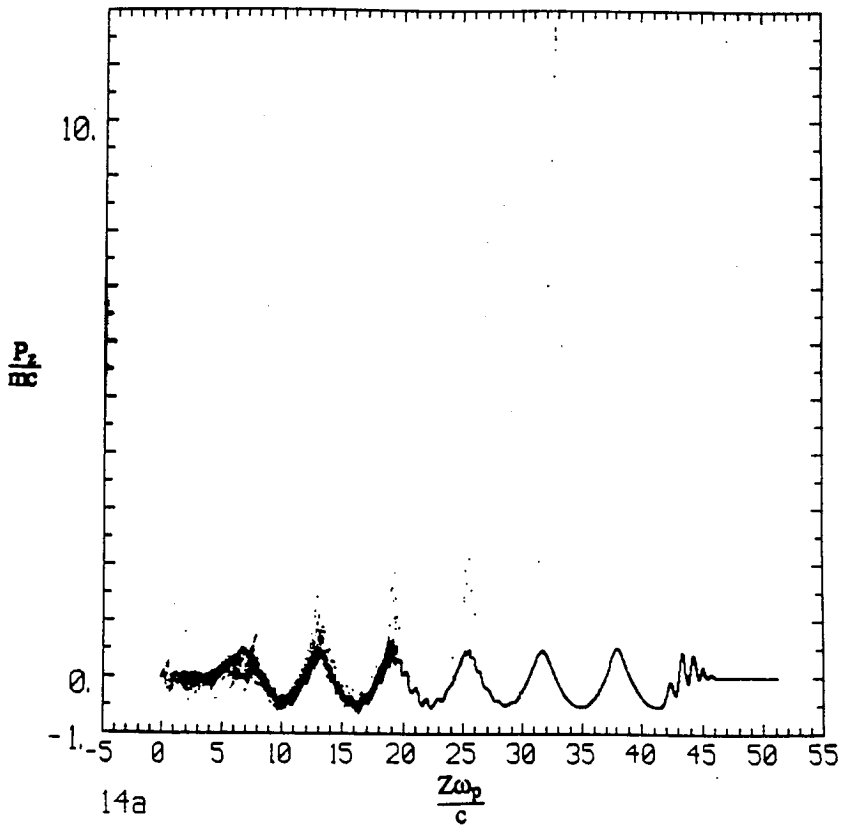

14. Same as Fig. 13 for a pulse amplitude of $0.6mc^2$.